Title page

Classification: Biological Sciences, Plant Biology

Title: A conserved but plant specific CDK-mediated regulation of DNA replication protein A2 in the precise control of stomatal terminal division*

Kezhen Yang[a], Lingling Zhu[a,b], Hongzhe Wang[a], Min Jiang[a], Chunwang Xiao[c,d], Xiangyang Hu[e], Steffen Vanneste[f,g,h], Juan Dong[i] and Jie Le[a,b,1]

[a] Key Laboratory of Plant Molecular Physiology, CAS Center for Excellence in Molecular Plant Sciences, Institute of Botany, Chinese Academy of Sciences, Beijing 100093, China. [b] University of Chinese Academy of Sciences, Beijing 100049, China. [c] College of Life and Environmental Sciences, Minzu University of China, Beijing 100081, China. [d] Hulun Lake Reserve Grassland Ecology Research Station, Minzu University of China, Beijing 100081, China. [e] Shanghai Key Laboratory of Bio-Energy Crops, School of Life Sciences, Shanghai University, Shanghai 200444, China. [f] VIB Center for Plant Systems Biology, Ghent 9052, Belgium. [g] Department of Plant Biotechnology and Bioinformatics, Ghent University, Ghent 9052, Belgium. [h] Laboratory of Plant Growth Analysis, Ghent University Global Campus, 21985 Incheon, Republic of Korea. [i] Waksman Institute of Microbiology, Rutgers, the State University of New Jersey, Piscataway, NJ 08854, USA.

[1] To whom correspondence should be addressed. Email: lejie@ibcas.ac.cn

* Dedicated to the memory of Fred Sack, who is a pioneer in the field of stomatal development.

Author contributions: K.Y. and J.L. designed the research and analyzed the data. K.Y. performed most of the experiments. L.Z. and W.H. contributed to the generation of some constructs. M.J. contributed to mutant screen. K.Y.,

J.L., J.D., X.H., S.V., and C.X. wrote the article.

Abstract:

The R2R3-MYB transcription factor FOUR LIPS (FLP) controls the stomatal terminal division through transcriptional repression of the cell cycle genes *CDKB1s*, *CDKA;1*, and *CYCA2s*. We mutagenized the weak mutant allele *flp-1* seeds with ethylmethane sulfonate (EMS) and screened out a *flp-1* suppressor 1 (*fsp1*) that suppressed the *flp-1* stomatal cluster phenotype. *FSP1* encodes RPA2a subunit of Replication Protein A (RPA) complexes that play important roles in DNA replication, recombination, and repair. Here, we show that *FSP1/RPA2a* functions together with *CDKB1s* and *CYCA2s* in restricting stomatal precursor proliferation, ensuring the stomatal terminal division, and maintaining a normal guard cell size and DNA content. Furthermore, we provide direct evidence for the existence of an evolutionally conserved, but plant-specific CDK-mediated RPA regulatory pathway. Serine-11 and Serine-21 at the N-terminus of RPA2a are CDK phosphorylation target residues. The expression of the phosphorylation-mimic variant $RPA2a^{S11,21/D}$ partially complemented the defective cell division and DNA damage hypersensitivity in *cdkb1;1 1;2* mutants. Thus, our study provides a mechanistic understanding of the CDK-mediated phosphorylation of RPA in the precise control of cell cycle and DNA repair in plants.

Keywords: Stomatal Development; Cell Division; Replication Protein A; CDK; DNA Damage

Significance:

The Arabidopsis R2R3-MYB transcription factor FOUR LIPS (FLP) is the first identified key transcription factor regulating stomatal development. By screening and analysis of a genetic suppressor of *flp* stomatal defects, we

found *FSP1/RPA2a*, encoding a core subunit of Replication Protein A (RPA) complexes, acts downstream of core cell cycle genes of CDKB1s in ensuring the terminal division during stomatal development to produce a pair of kidney-shaped guard cells to compose a functional stomatal complex. We demonstrate that the CDK-mediated phosphorylation at the N-terminus of RPA2a is essential for the RPA functions in cell cycle control and response to DNA damage. We provide the direct evidence for the existence of an evolutionally conserved, but plant-specific RPA regulatory pathway in plants.

\body

Introduction

Stomata are plant-specific epidermal structures that consist of a pair of Guard Cells (GCs) surrounding a pore. The formation of stomata requires successive asymmetric cell division of the precursor cells, including the Meristemoid Mother Cell (MMC) and the Meristemoid (M), and one symmetric division of the Guard Mother Cell (GMC) to produce two GCs (1). *FOUR LIPS* (*FLP*) and *MYB88* encode R2R3-MYB transcription factors and function in the regulation of symmetric division of the GMCs. In a weak allele *flp-1*, two stomata form abnormally in direct contact. The loss of *MYB88* function dramatically enhances the phenotype of *flp* mutants, leading to tumor-like stomatal clusters (2, 3). The cell cycle genes *CDKB1s*, *CYCA2s,* and *CDKA;1,* as transcriptional targets, are directly suppressed by FLP and MYB88 (4-6).

Replication Protein A (RPA) is a heterotrimeric single-stranded DNA (ssDNA)-binding protein complex that is required for multiple aspects of DNA metabolism, including DNA replication, recombination, repair, and telomere maintenance (7). The homologues of each of the three RPA subunits (RPA1-3) are well conserved in eukaryotes. In humans, phosphorylation of

RPA2 at the N-terminal domain is required for the RPA-ssDNA interaction. In mitotic cells, Serine-23 and Serine-29 at the RPA2 N-terminus are phosphorylated and activated by Cdc2/CDK to promote DNA replication (8-12). Upon a DNA damaging condition, RPA2 is hyperphosphorylated by the PIKK-family kinases (ATM, ATR, and DNA-PK) that facilitates mitotic exit and the initiation of DNA repairing (13-15). All known RPA2 homologues have a conserved N-terminal phosphorylation domain, though the specific residues may be not conserved in different species (11). In contrast to yeast and most mammals, plants carry multiple paralogs for each of the RPA subunit (16). For instance, rice has three RPA1s, three RPA2s, and one RPA3 (16, 17). The model plant Arabidopsis has five RPA1s (RPA1a-e), two RPA2s (RPA2a, b), and two RPA3s (RPA3a, b). Phylogenetic analysis of the RPA1 sequences suggests that Arabidopsis RPA1s diverged into two subgroups, the ACE-group (RPA1a, b, c) and the BD-group (RPA1b, d) (18). Previously, genetic analysis confirmed that *RPA2a* plays a critical role in the maintenance of epigenetic gene silencing in plants and abiotic stresses (19-21).

In this study, with an aim of obtaining genetic suppressors of *flp-1*, we identified a genetic mutation in Arabidopsis *RPA2a* that led to inhibited stomatal clustering in *flp-1* and arrested GMC divisions. Our study discovered the existence of an evolutionally conserved, but plant-specific CDK-mediating RPA regulatory pathway. Also, by assaying the stomatal development and DNA damage responses, we established the physical and genetic interactions between the RPA and CDKs in the precise control of cell cycle as well DNA repair in plants.

Results

Isolation of *fsp1,* a Suppressor of *flp-1* in Stomatal Development. The

flp-1 mutant is featured by extra terminal divisions during stomatal development, suggesting the role of FLP in restricting cell division (3). To identify new genetic players in regulating the one-time terminal division, we created an ethylmethane sulfonate (EMS) mutagenized M2 population of *flp-1* mutants and screened for mutants with altered stomatal phenotypes. *flp-1 fsp1* (*flp-1 s*uppressor1) was isolated for significantly reduced stomatal clusters, compared to *flp-1* (Fig.1 *A*-*C* and *SI Appendix,* Table S1). In addition, aberrant cells were occasionally found in the epidermis of *flp-1 fsp1* double mutant (Fig. 1*C*). Using a GC fate marker E1728, we confirmed that the aberrantly shaped, single cells in *fsp1* have the GC identity (Fig. 1D and inset), resembling the Single Guard Cell (SGC) phenotype in *cdkb1;1 1;2* and *cyca2s* mutants (4,5). The Stomatal Index (SI) of *fsp1* mutant was reduced as well, indicating that *FSP1* promotes stomatal production (*SI Appendix,* Table S2).

***FSP1* Encodes Arabidopsis RPA2a Subunit of the RPA Complex.** Using map-based cloning, we determined that mutation of *FSP1* gene was located within the BAC clone T28124 on chromosome 2. Based on growth defects reminiscent of *rpa2a/ror1-1* mutants, such as dwarf seedlings, narrow leaves, and early flowering (*SI Appendix,* Fig. S1*A*) (19, 20), we amplified and sequenced the open reading frames of *RPA2a* from *fsp1* and found that *fsp1* possessed the same point mutation as in *ror1-2,* ag (1343) changed to aa, which induces altered splicing events (Fig. 1*E*). The expression of *RPA2a* (cDNA) fused with GFP under the control of the native promoter fully rescued the stomatal defects of *fsp1* mutants (Fig. 1*F* and *SI Appendix,* Table S2). The functionality of *RPA2a* was further confirmed by the reappearance of *flp-1*-featured stomatal clusters in *flp-1 fsp1* mutants carrying *RPA2a:RPA2a-GFP* (Fig. 1*G* and *SI Appendix,* Table S1). In addition, the introgression of the *fsp1* mutation in *flp-1 myb88* double mutants largely

repressed the size and number of stomatal clusters (Fig. 1 *H,I* and *SI Appendix,* Fig. S1*B*). We also revisited the T-DNA allele, *rpa2-5/ror1-3* (Fig. 1*E* and *SI Appendix,* Fig. S1*A*) (19, 20), which displayed a similar stomatal phenotype as *fsp1.* The *flp-1* stomatal phenotype was suppressed in *flp-1 rpa2-5* double mutants (*SI Appendix,* Fig. S1 *C,D* and Table S2). Benefiting from easy genotyping, *rpa2-5* was then used in most of the later experiments (renamed as *rpa2a-5*).

***RPA2a* Is Expressed in Specific Stomatal Lineage Stages.** A complemented *ror1-1* transgenic line harboring *ROR1:gROR1-GUS-GFP* (19) (here referred as *RPA2a-GFP*) was used to investigate the RPA2a expression pattern and localization. RPA2a-GFP fluorescent signals were observed in a subset of stomatal lineage cells and compared with those of three translational reporters of *SPEECHLESS* (*SPCH)*, *MUTE,* and *FLP*, which have distinct and sequential expression patterns during stomatal development (Fig. 1*J*). The expression of RPA2a-GFP overlapped with *SPCH-GFP* (22) in MMCs prior to asymmetric entry divisions but not in both newly-formed meristemoids (M) and Stomatal Lineage Ground Cells (SLGC) after division. In late meristemoids and early GMCs (EGMCs), where MUTE-GFP was turned on (23), diffuse RPA2a-GFP signals reappeared. RPA2a-GFP persisted in late GMCs (LGMCs), but disappeared in young GCs (YGCs) after the terminal symmetric cell division. The expression of *RPA2* overlapped with *FLP-GFP* (3, 24) only at LGMC stage, prior to the GMC division, but not in YGCs. Taken together, *RPA2a* shows a cell type- and time-specific expression profile, with the preferences in the precursor cells (actively dividing) prior to either asymmetric or symmetric divisions during stomatal development.

***RPA2a* Functions Together with FLP Downstream Target Genes *CDKB1s* and *CYCA2s*.** *CDKB1;1* gene is one of the direct transcriptional

targets of FLP in controlling stomatal terminal symmetric divisions. In agreement with this, expression of *CDKB1;1-GFP* (24) overlaps with *FLP-GFP* in LGMCs and YGCs while partially with *RPA2a-GFP* in LGMCs (Fig. 1*J*). In comparison to SGC frequencies of 42.0 ± 2.6% in *cdkb1;1 1;2* and 8.0 ± 2.1% in *rpa2a-5,* the *rpa2a-5 cdkb1;1 1;2* triple mutant produced dramatically more SGCs (64.0 ± 1.6%, Fig. 2*A-D*). GMC divisions also require *CYCA2* activity (5). While SGCs in *cyca2;3* mutants was found at a low frequency of 4.0 ± 0.8% (Fig. 2*E*), the occurrence of SGCs in *rpa2a-5 cyca2;3* double mutants was elevated to 47.0 ± 2.0% (Fig. 2*F*). Consistently, the frequency of SGCs in *cyca2;3 2;4* (27.6 ± 3.4%) was greatly elevated to 78.0 ± 8.5% in *rpa2a-5 cyca2;3 2;4* triple mutants (Fig. 2 *G* and *H*), indicating interaction between RPA2a and CDKB1s/CYCA2s functions in GMC divisions.

An ectopic and prolonged expression of RPA2a-GFP was occasionally found in two daughter cells after a GMC division in *flp-1,* suggesting that RPA2a is required for subsequent GMC divisions that end up with two stomata next to each other (*SI Appendix,* Fig. S2 *A-H*). *RPA2a* transcription level slightly but not significantly increased in *flp-1 myb88* (*SI Appendix,* Fig. S2*I*). Although 12 putative FLP/MYB88 binding sequences are present within the *RPA2a* promoter (4-6), neither FLP nor MYB88 showed clear binding activity to *RPA2a* promoter according to the results of yeast one-hybrid assays (*SI Appendix*, Fig. S2 *J* and *K*), indicating that *RPA2a* might not be a direct transcriptional target of FLP/MYB88.

Combined Loss of *RPA2a* and *CDKB1s/CYCA2s* Function Induces Abnormal Cell Enlargement and Endoreduplication. Differing from the interlocking, continuously expanding pavement cells, the mature stomatal GCs once matured remain their shape and size for the life time in leaves. The area of the paired GCs mostly ranged from 200 to 500 μm^2 in

Arabidopsis (*SI Appendix,* Fig. S3). However, about 45% and 71% stomata in *rpa2a-5 cdkb1;1 1;2* and *rpa2a-5 cyca2;3 2;4* triple mutants, respectively, are larger than 500 μm^2 (Fig. 2 *A*-*H* and *SI Appendix,* Fig. S3). It has been widely accepted that cell size and differentiation are closely correlated to the nuclear DNA levels (25). We therefore measured the nuclear DNA levels in SGCs after DAPI (4′,6-diamidino-2-phenylindole) staining. The DNA content in wild-type GCs was defined as 2C-DNA level. Our results showed that SGCs in the *rpa2a-5, cdkb1;1 1;2,* and *cyca2;3 2;4* mutants all displayed a similar DAPI fluorescence intensity (4C-DNA level), indicating that *RPA2a*, similar to *CDKB1s* and *CYCA2s*, is required for the mitosis of GMC divisions. But in the *rpa2a-5 cdkb1;1 1;2* or *rpa2a-5 cyca2;3 2;4* triple mutants, the enlarged SGCs contained single giant nuclei with a mean DNA level of 6C-8C (Fig. 2 *I*-*N*). The analysis of DNA ploidy distribution in 9- and 14-day-old cotyledons using flow cytometry confirmed that RPA2a may coordinately act with CDKB1s/CYCA2s to restrict the onset of endocycle (*SI Appendix,* Fig. S4).

Above results indicated that the mitosis was blocked but the endoreplication was inappropriately unrestricted in the *rpa2a-5 cdkb1;1 1;2* triple mutants. In *rpa2a-5* single mutant, the expression levels of G1-to-S genes *CDT1*, *MCM2*, *ORC3*, and *PCNA1* were significantly increased comparing those in wild type. Most of these elevations as well as *CDC6a*, *CCS52A*, *ORC1a*, *CDKA;1,* were additively enhanced in *rpa2a-5 cdkb1;1 1;2* triple mutants (*SI Appendix,* Fig. S5*A*). In addition, the expression levels of genes during endoreplication initiation, such as *E2Fa*, *E2Fc*, and *E2Ff,* were largely increased in the triple mutants (*SI Appendix,* Fig. S5*B*). These results demonstrated that RPA2a and CDKB1s act together to suppress the expression of endocycling genes that restrict endoreduplication.

RPA2a Function Is Conservatively Regulated by CDKs through Protein

Phosphorylation. Supported by our genetic data above, we tested the hypothesis that RPA2a may directly interact with CDKs in regulating cell division and cell cycle. Results of Bimolecular Fluorescent Complementation (BiFC) assays using the tobacco transient expression system and Co-ImmunoPrecipitation (Co-IP) assay using the proteins that were extracted from the infiltrated tobacco leaves suggested that RPA2a directly interacts with CDKB1;1 and CDKA;1 (Fig. 3 *A-D* and *SI Appendix,* Fig. S6).

It was reported that coexpression of the RPA2 subunit with other RPA subunits could enhance the solubility and function of RPA protein complexes (26). When RPA2a-GST was coexpressed with RPA1b-HIS in *E. coli,* RPA1b proteins failed to be pulled down by RPA2a. Only when the RPA3a was present, in which RPA2a-GST-RPA3a-S coexpressed with RPA1b-HIS, the whole RPA complex could be pulled down by GST beads, indicating that the pre-formation of RPA2-RPA3 subcomplex is essential for the assembly of RPA complex (*SI Appendix,* Fig. S7*A*). However, regardless the presence of RPA3 and RPA1, RPA2a proteins could be phosphorylated *in vitro* by active CDK-CYCLIN protein complexes (27) (Fig. 3 *E,F and SI Appendix,* Fig. S7*B*). Additionally, a faint delayed band next to the RPA2a-GST was observed when the products of CDK phosphorylation reaction were separated on SDS-PAGE gels (Fig. 3*G*). Once alkaline phosphatases were added to the products, the delayed band disappeared, indicating the phosphorylation is the cause of the slower mobility of RPA2a-GST proteins in gels (*SI Appendix,* Fig. S7*B*). Elimination of the N-terminal 32 amino acids abolished the delayed band, suggesting that this region contains the primary phosphorylation target sites (Fig. 3*G*).

To predict the CDK-phosphorylation target residues in RPA2a protein, the sequence of the N-terminus of RPA2a protein was compared with those in human, yeast, and rice RPA2 proteins. Among the 12 Serine residues within

the first 32 amino acids of RPA2a N-terminus, Ser-11 is the consensus CDK phosphorylation sites, corresponding to Ser-23 of human RPA2 protein. Ser-21 is another predicted phosphorylation target site of CDKs (www.cbs.dtu.dk/services/) that maybe conserved in plants (*SI Appendix,* Fig. S7 *C-F*). When Ser-11 and Ser-21 were substituted with non-phosphorylatable Glycines, the extent of phosphorylated band was reduced (Fig. 3*G*), indicating that these two residues are predominant CDK-phosphorylation targets, but other sites in RPA2a might get phosphorylated *in vitro* as well.

To assess the function of phosphorylation sites in the RPA2a protein *in planta*, RPA2a variants were generated and introduced into *rpa2a-5* mutant to evaluate their ability to rescue stomatal defects. *RPA2a-GFP*, and individual variants with single mutation, *RPA2a*$^{S11/G}$*-GFP* and *RPA2a*$^{S21/G}$*-GFP*, could fully rescue the stomatal production and GMC division defects of *rpa2a-5* mutant (*SI Appendix,* Table S2). By contrast, further mutation of *RPA2a*$^{S11,21/G}$*-GFP* or N-terminus deletion variant *RPA2a*$^{\triangle 32}$*-GFP* showed a reduced rescuing ability (Fig. 4 *A*, *B* and *SI Appendix,* Table S2). However, a phosphorylation-mimic variant *RPA2a:RPA2a*$^{S11,21/D}$*-GFP* (Ser-11 and Ser-21 were substituted with Aspartic acids) rescued *rpa2a-5* GMC division defects (Fig. 4*C* and *SI Appendix,* Table S2).

We further examined how RPA2a phosphorylation-variants perform in *flp-1 fsp1* double mutants. While, the wild-type RPA2a-GFP fully complemented the loss function of *RPA2a* and restored the *flp-1*-like stomatal clustering, the expression *RPA2a:RPA2a*$^{\triangle 32}$*-GFP* and *RPA2a:RPA2a*$^{S11,21/G}$*-GFP* led to a mild stomatal clustering phenotype (Fig. 4 *D* and *E* and *SI Appendix,* Table S1). *RPA2a*$^{S11/G}$*-GFP* and *RPA2a*$^{S21/G}$*-GFP* fully complemented stomatal phenotype of *flp-1 fsp1* (*SI Appendix,* Table S1). Therefore, the

phosphorylation status of Ser-11 and Ser-21 within the N-terminal 32 residues is critical for the full function of RPA2a.

We introduced *RPA2a-GFP*, *RPA2a:RPA2a*$^{S11/D}$*-GFP*, *RPA2a*$^{S21/D}$*-GFP*, and *RPA2a*$^{S11,21/D}$*-GFP* into *cdkb1;1 1;2* double mutants to assess the genetic interaction between *RPA2a* and *CDKB1s in vivo*. *RPA2a*$^{S11,21/D}$*-GFP* showed strong effects in reducing the formation of SGCs in *cdkb1;1 1;2*, while the remaining three transgenes had certain effects (Fig. 4 *F-H* and *SI Appendix,* Table S3). Therefore, these results suggest that the phosphorylation status of RPA2a is epistatic to *CDKB1* mutations.

CDKB1 Activity Promotes RPA2a Nuclear Localization. The strong expression of complementary RPA2a-GFP was mainly found in the nucleus, but also present in the cytoplasm. RPA2a-GFP signals were more diffuse in *cdkb1;1 1;2* epidermal cells (Fig. 5 *A*,*B* and *SI Appendix,* Fig. S8 *A* and *B*). Western blot analysis confirmed the abundance of nuclear RPA2a-GFP proteins was decreased in *cdkb1;1 1;2* (Fig. 5*C*). RPA2a$^{\Delta 32}$-GFP and the phosphorylation-deficient version RPA2a$^{S11,21/G}$-GFP displayed a pronounced fluorescent signals in the cytoplasm of epidermal cells (Fig. 5 *D*, *E* and *SI Appendix,* Fig. S8 *C* and *D*). By contrast, the signals of RPA2a$^{S11,21/D}$-GFP, which fully complemented the stomatal defects of *rpa2a-5*, displayed a high degree of colocalization with DAPI in the nucleus, with a Pearson's-Rr value of 0.89 (Fig. 5*F* and *SI Appendix,* Fig. S8*E*). Quantitative analysis of relative GFP fluorescent intensity in the nucleus consistently supported that CDK-mediated phosphorylation of RPA2a promotes the nuclear accumulation of RPA2a (*SI Appendix,* Fig. S8*K)*.

We fused the Nuclear Localization Sequence (NLS) or Nuclear Export Signal (NES) to the C-terminus of CDKB1;1 and co-expressed with RPA2a-mCherry in tobacco leaves. A Non-Nuclear Localization Sequence (NNLS, a control

sequence to the NLS) and Non-Nuclear Export Signal (NNES, a control sequence to the NES) (28) were also fused with CDKB1;1 as controls. When individually expressed, RPA2a-mCherry remained in nucleus and cytoplasm (*SI Appendix,* Fig. S9*A*). However, RPA2a-mCherry signals predominantly retained in the nucleus when co-expressed with CDKB1;1-NLS-GFP (*SI Appendix*. Fig. S9*B*). By contrast, when co-expressed with CDKB1;1-NES-GFP, besides the nucleus, abundant RPA2a-mCherry signals were accumulated in the cytoplasm (*SI Appendix* Fig. S9*C*). CDKB1;1-NNLS-GFP or CDKB1;1-NNES-GFP did not change the subcellular localization pattern of RPA2a-mCherry (*SI Appendix* Fig. S9 *D* and *E*). Thus, the physical interaction with CDKB1;1 either in the nucleus or in the cytoplasm seems to affect the subcellular localization of RPA2a.

To further clarify whether the subcellular localization is associated with the function of RPA2a, we generated NLS-fused *RPA2a:RPA2a-NLS-GFP,* and NES-fused *RPA2a:RPA2a-NES-GFP* and transformed into *rpa2a-5* mutant. The fluorescent signals of RPA2a-NLS-GFP were exclusively accumulated in the nuclei (Fig. 5*H* and *SI Appendix,* Fig. S8 *G* and *L*), in which the defective overall growth and GMC division of *rpa2a-5* mutants were fully recovered (Fig. 5*L* and *SI Appendix,* Table S4). However, a transgenic line carrying *RPA2a-NES-GFP* line #12, in which the diffuse GFP signals were detected in both cytoplasm and nucleus (Fig. 5*J* and *SI Appendix,* Fig. S8 *I* and *L)*, the growth and stomatal defects in *rpa2a-5* were partially rescued (Fig. 5*L* and *SI Appendix,* Table S4). Whereas, *RPA2a-NES-GFP* transgenic line #5, in which GFP signals were mostly restricted to the cytoplasm, showing a barely colocalization with DAPI in the nucleus, a representative low value of Pearson's-Rr at -0.23 (Fig. 5*K* and *SI Appendix,* Fig. S8*J* and *L*). Neither the plant growth defect nor the stomatal defect of *rpa2a-5* mutant was rescued in line #5 (Fig. 5*L* and *SI Appendix,* Table S4). The high expression level of

RPA2a-NES-GFP in line #5 (*SI Appendix,* Fig. S10) might provide higher nuclear export signals (from the NES), which drive RPA2a proteins into the cytoplasm against the endogenous nuclear 'stay force', such as being phosphorylated by CDKs. The control lines *RPA2a-NNLS-GFP* and *RPA2a-NNES-GFP* phenocopied the protein localization and complementation ability of the wild-type RPA2a-GFP (Fig. 5 *G*, *I*, *L* and *SI Appendix,* Fig. S8 *F*, *H* and Table S4).

The N-terminal Domain Is also Required for RPA2a's Function in Response to DNA Damage. It has been reported that Arabidopsis *rpa2a* alleles exhibited hypersensitivity to the genotoxic agent Methyl Methane Sulfonate (MMS) treatment (19-21). However, how the RPA2a protein and its subdomains are related to the DNA damage responses in plants remains unknown. The 5-day MMS treatment generally arrested plant growth and induced seedling chlorosis. The introduction of *RPA2a-GFP* or *RPA2a*$^{S11,21/D}$*-GFP* recovered *rpa2a-5* growth to the wild-type level. However, the N-terminal defectives RPA2a$^{\triangle 32}$-GFP and phosphorylation-deficient RPA2a$^{S11,21/G}$-GFP only partially complemented the chlorosis phenotype of *rpa2a-5* (*SI Appendix,* Fig. S11). Furthermore, *cdkb1;1 1;2* and *rpa2a-5 cdkb1;1 1;2* displayed hypersensitivity to MMS treatment as well. The phosphorylation-mimic variant RPA2a$^{S11,21/D}$ alleviated the sensitivity of *cdkb1;1 1;2* to MMS (Fig. 6 *A,B* and *SI Appendix,* Fig. S12), that is consistent with its stronger capability than wild-type RPA2a in rescuing *cdkb1;1 1;2* GMC divisions (*SI Appendix,* Table S3). Therefore, our finding observation is consistently with the previous findings in yeast and human that the phosphorylation of N-terminus is important for RPA2 function in response to DNA damage.

Discussion

In this study, we found that a genetic mutation in Arabidopsis *RPA2a* not only suppressed *flp-1* stomatal clustering phenotype but also induced the formation of SGCs. *RPA2a* functions together with *CDKB1s* and *CYCA2s* in ensuring the stomatal lineage cell divisions and maintaining a normal DNA content and guard cell size. Furthermore, we found that Ser-11 and Ser-21 of Arabidopsis RPA2a are consensus sites for CDK phosphorylation. Being phosphorylated by CDKs at these sites is tightly associated with the RPA2a subcellular localization and function in cell cycle control and the response to DNA damage.

RPA2a and Core Cell Cycle Genes Coordinately Control Cell Cycle Procession. FLP and MYB88 directly repress the transcription of several core cell cycle genes, such as *CDKB1;1*, *CYCA2;3*, and *CDKA;1*, to ensure that only two GCs are produced during the terminal GMC divisions (2-6). FLP, as an atypical R2R3-MYB transcription factor, recognizes downstream targets through a *cis*-regulatory element that overlaps with E2Fs (4, 33, 34). There are 12 putative FLP/MYB88/E2F binding sequences within the *RPA2a* promoter. But, neither FLP nor MYB88 displayed a clear binding activity to the *RPA2a* promoter (*SI Appendix,* Fig. S2). It was proposed that rice *OsRPA1* and *OsRPA2* might be the target genes of the S-phase transcription factor E2Fs (35). It will be interesting to test whether FLP and MYB88 compete with E2Fs in regulating *RPA2a* transcription.

RPA stabilizes ssDNA and interacts with replication proteins at the initiation site of DNA replication to facilitate the formation of replication forks (12, 36). CDT1 and CDC6 are DNA replication licensing components that help the loading of the MCM DNA helicases to the DNA replication origins. Similar to human Cdt1 proteins, the Arabidopsis CDT1 is degraded through a CDK-mediated phosphorylation. *CDT1* and *CDC6* are also regulated by E2F transcription factors (37). In *rpa2a cdkb1;1 1;2* or *rpa2a cyca2;3 2;4*,

transcription levels of a set of G1-to-S phase genes, including *CDT1, CDC6, E2F*-family genes are significantly upregulated, indicating that *RPA2a* and core cell cycle genes coordinately restrict the G1-to-S transition and prevent the entry of endocycle. Recently, the roles of *CYCD5;1* and *CYCD7;1* in regulating GMC division and differentiation have been elegantly described (38, 39). However, the expression of *CYCD5;1* and *CYCD7;1* was not altered either in *rpa2a-5, cdkb1;1 1;2* or in *rpa2a-5 cdkb1;1 1;2* triple mutants (*SI Appendix*, Fig. S5*C*).

The Functions of RPA2a Are Regulated by CDKs in Plant-specific Manner. RPA2 proteins get phosphorylated during the G1-to-S transition and M-phase, dephosphorylated at the end of M-phase (8, 29-31). In yeast, a single CDK (cdc2) regulates DNA replication licensing, DNA replication initiation, and cell mitosis by changing its activity levels from low, to intermediate and high, respectively (38, 40). CDK-mediated RPA2 phosphorylation at Ser-23 occurs during S-phase while phosphorylation at Ser-29 happens only during mitosis (12). In Arabidopsis, generally, CDKA;1 activity is more important for the G1-to-S transition, CDKB1s is required for the G2-to-M progression (32). Here, we found that RPA2a proteins could be phosphorylated by CDKA;1 *in vitro* as well, suggesting that RPA2a might be regulated by both A1- and B1-type CDKs in Arabidopsis. Therefore, in contrast to the single CDK in yeast, the divergent functions of RPA2a from DNA replication to mitosis might by regulated by both A1-type CDKA;1 and the plant specific B1-type CDKB1s (Fig. 6*C*).

RPA2a and CDK-CYCLIN Are Involved in DNA Repair. DNA Double-Strand Breaks (DSBs) also can occur during DNA replication. Arabidopsis *atm* mutant displays chromosomal fragmentation and reduced fertility (41). SUPPRESSOR OF GAMMA RESPONSE 1 (SOG1) is a functional analogue of mammalian tumour suppressor p53 in plants, which is

directly phosphorylated and activated by ATM upon DNA damage (42, 43). The activated SOG1 induces an increase of *CYCB1;1* transcript (44). In *rpa2a-5*, the transcription level of *CYCB1;1*, but not *CYCA2;3*, was dramatically upregulated (*SI Appendix,* Fig. 12*B*), suggesting the existing of a regulatory circuit during DNA repair.

Materials and Methods

Details on plant growth conditions, positional cloning, plasmid construction, flow cytometric analysis, protein-protein interaction BiFC and Co-IP assays are provided in *SI Appendix, Materials and Methods*.

ACKNOWLEDGMENTS. We thank Fred Sack for providing the *flp* and *CDKB1;1-GFP* seeds, Dominique Bergmann for *SPCH* and *MUTE* markers, Arp Schnittger for the plasmids of CDKA;1 and CDKB1;1 kinase complexes, Daniela Kobbe for the plasmids for RPA complexes, Zhizhong Gong for *ror1* and *ROR1-GFP* seeds, Chongyi Xu for helps in Co-IP experiments and Lu Wang for editing. This work was supported by grants from the National Natural Science Foundation of China program 31071198 (K.Y.), 30971652 and 31271463 (J.L.), 31470348 (X.H.), and a Cooperative Programme between National Natural Science Foundation of China (NSFC) - Research Foundation Flanders (FWO) to J.L. and S.V. The research projects in J.D.'s lab are supported by the NIH R01GM109080.

Figure legends:

Fig. 1. *FSP1* encodes RPA2a subunit required for stomatal precursor cell divisions. (*A-D*) DIC images of epidermis of wild-type (*A*), *flp-1* (*B*), *flp-1 fsp1*(*C*), and *fsp1* (*D*). Brackets indicate the stomatal clusters. SGCs are highlighted with yellow color and normal GCs with blue color. Inset, expression of the mature GC marker E1728 in a SGC. (*E*) Map-based isolation and gene structure of *FSP1*. The mutation site in *fsp1* is the same as *ror1-2*. *rpa2a-5* (*ror1-3*) is a T-DNA insertion line. (*F* and *G*)

RPA2a:RPA2a-GFP rescued *fsp1* SGC phenotype (*F*), while induced the reappearance of *flp-1* clusters in *flp-1 fsp1* (*G*). (*H* and *I*) *flp-1 myb88* cluster numbers and size are repressed by *fsp1* mutation. (*J*) *RPA2a-GFP* expression profile in the stomatal linage cells. RPA2a-GFP (Scale bars: 20 μm).

Fig. 2. RPA2a function synergistically with CYCA2s and CDKB1s in GMC division. (*A*-*G*) Micrographs of epidermis of wild-type (*A*), *rpa2a-5* (*B*). *cdkb1;1 1;2* (*C*), *rpa2a-5 cdkb1;1 1;2* (*D*), *cyca2;3* (*E*), *rpa2a-5 cyca2;3* (*F*), *cyca2;3 2;4* (*G*), and *rpa2a-5 cyca2;3 2;4* (*H*). SGCs are highlighted with yellow color and normal GCs with blue color. The numbers at the right-upper corner indicate percentage of SGCs in total stomata. (*I*-*N*) DAPI fluorescence micrographs. Red arrowheads indicate the nuclei. (Scale bar: 20 μm).

Fig. 3. Phosphorylation of RPA2a by CDK complexes. (*A*-*D*) The RPA2a protein binds CDKB1;1 protein in BiFC assays (*A*-*C*) and Co-IP assays (D). (Scale bars: 20 μm). *(E*) *in vitro* phosphorylation assays. RPA2a is phosphorylated by Cak1-CDKA;1-CYCD3;1 complex in the form of RPA1b-RPA2a-RPA3a complex. (*F*) RPA2a is also phosphorylated by Cak1-CDKB1;1-CYCB1;2 complexes. The bottom box shows the loading controls after Coomassie Brilliant Blue (CBB) gel staining. MBP and GST proteins were used as positive and negative controls, respectively. Red arrows, the RPA2a phosphorylation band in phosphorylation autoradiographs. (G) Phosphorylation of RPA2a by Cak1-CDKB1;1-CYCB1;2 complexes is confirmed by finding a delayed band in 12.5% SDS-PAGE. The extent of phosphorylation of the RPA2a proteins was reduced when Ser-11 and Ser-21 were substituted or was barely detected when the N-terminus was deleted.

Fig. 4. Rescue stomatal phenotypes by *RPA2a* variants. (*A*-*C*) The formation

of SGCs in *rpa2a-5* mutant was partially rescued by *RPA2a*$^{\triangle 32}$*-GFP* construct (*A*) or *RPA2a*$^{S11,21/G}$*-GFP* (*B*), while was mostly rescued by *RPA2a*$^{S11,21/D}$*-GFP* (*C*). (*D* and *E*) The formation of SGCs in *flp-1 fsp1* was barely affected by *RRPA2a*$^{\triangle 32}$*-GFP* (*D*) or *RPA2a*$^{S11,21/G}$*-GFP* (*E*). (*F-H*) The formation of SGCs in *cdkb1;1 1;2* mutant is partially rescued by *RPA2a-GFP* (*G*), but is greatly repressed by *RPA2a*$^{S11,21/D}$*-GFP* (*H*). The numbers at the right-upper corner indicate percentage of SGCs in total stomata. SGCs are highlighted with yellow color and normal GCs with blue color. (Scale bars: 10 μm).

Fig. 5. Function of RPA2a is associated with its phosphorylation status and subcellular localization. (*A*) Nuclear expression of RPA2a-GFP in a complemented *rap2a-5*. (*B*) Diffuse RPA2a-GFP in *cdkb1;1 1;2*. (*C*) RPA2a-GFP proteins were found in both the cytoplasm and the nucleus by western blot analysis. Amount of RPA2a-GFP in the nucleus is reduced in *cdkb1;1 1;2*. (*D* and *E*) Diffuse GFP signals in RPA2a$^{\triangle 32}$-GFP (*D*) and RPA2a$^{S11,21/G}$-GFP (*E*). (*F*) Predominant GFP signals in the nucleus of RPA2a$^{S11,21/D}$-GFP. (*G-K*) The RPA2a subcellular localization in RPA2a-NNLS-GFP (*G*), RPA2a-NLS-GFP (*H*), RPA2a-NNES-GFP (*I*), and two RPA2a-NES-GFP transgenic lines, line #12 (*J*) and line #5 (*K*). Insets, the enlarged region highlighted by the white dashed-line boxes. (Scale bars: 20 μm). (*L*) The retarded overall growth of *rpa2a-5* was rescued by *RPA2a* variants except *RPA2a-NES-GFP.* (Scale bar: 1 cm).

Fig. 6. Phosphorylation-mimic *RPA2a*$^{S11,21/D}$ alleviated the MMS effects in *cdkb1;1 1;2.* (*A* and *B*) Seven-day-old seedlings were transferred to liquid MS (*A*) or liquid MS medium containing 0.01% MMS (*B*) for 5 days before imaging. Seedlings of *rpa2a-5*, *cdkb1;1 1;2*, and *rpa2a-5 cdkb1;1 1;2* displayed hypersensitivity to MMS. Phosphorylation-mimic *RPA2a*$^{S11,21/D}$

alleviated the MMS effects on *cdkb1;1 1;2*. (Scale bar: 1 cm). (*C*) Model for RPA2 function in stomatal terminal division regulation and DNA repair progression. T-bars and dashed-lines indicate negative and positive regulation, respectively.

References

1. Bergmann DC & Sack FD (2007) Stomatal development. *Annu Rev Plant Biol* 58(1):163-181.
2. Yang M & Sack FD (1995) The *too many mouths* and *four lips* mutations affect stomatal production in *Arabidopsis*. *Plant Cell* 7(12):2227-2239.
3. Lai LB*, et al.* (2005) The Arabidopsis R2R3 MYB proteins FOUR LIPS and MYB88 restrict divisions late in the stomatal cell lineage. *Plant Cell* 17(10):2754-2767.
4. Xie Z*, et al.* (2010) Regulation of cell proliferation in the stomatal lineage by the Arabidopsis MYB FOUR LIPS via direct targeting of core cell cycle genes. *Plant Cell* 22(7):2306-2321.
5. Vanneste S*, et al.* (2011) Developmental regulation of CYCA2s contributes to tissue-specific proliferation in Arabidopsis. *EMBO J* 30(16):3430-3441.
6. Yang K*, et al.* (2014) Requirement for A-type cyclin-dependent kinase and cyclins for the terminal division in the stomatal lineage of Arabidopsis. *J Exp Bot* 65(9):2449-2461.
7. Wold MS (1997) Replication protein A: a heterotrimeric, single-stranded DNA-binding protein required for eukaryotic DNA metabolism. *Annu Re Biochem* 66:61-92.
8. Dutta A & Stillman B (1992) cdc2 family kinases phosphorylate a human cell DNA replication factor, RPA, and activate DNA replication. *EMBO J* 11(6):2189-2199.
9. Henricksen LA, Carter T, Dutta A, & Wold MS (1996) Phosphorylation of human replication protein A by the DNA-dependent protein kinase is involved in the modulation of DNA replication. *Nucleic Acids Res* 24(15):3107-3112.
10. Niu H*, et al.* (1997) Mapping of amino acid residues in the p34 subunit of human single-stranded DNA-binding protein phosphorylated by DNA-dependent protein kinase and Cdc2 kinase in vitro. *J Biol Chem* 272(19):12634-12641.
11. Binz SK, Lao Y, Lowry DF, & Wold MS (2003) The phosphorylation domain of the 32-kDa subunit of replication protein A (RPA) modulates RPA-DNA interactions. Evidence for an intersubunit interaction. *J Biol Chem* 278(37):35584-35591.
12. Oakley GG & Patrick SM (2010) Replication protein A: directing traffic at the intersection of replication and repair. *Frontiers in bioscience : a journal and virtual library* 15:883-900.
13. Oakley GG*, et al.* (2003) RPA phosphorylation in mitosis alters DNA binding and protein-protein interactions. *Biochemistry* 42(11):3255-3264.
14. Anantha RW, Sokolova E, & Borowiec JA (2008) RPA phosphorylation facilitates mitotic exit in response to mitotic DNA damage. *Proc Natl Acad Sci USA*

105(35):12903-12908.
15. Anantha RW & Borowiec JA (2009) Mitotic crisis: the unmasking of a novel role for RPA. *Cell cycle* 8(3):357-361.
16. Aklilu BB & Culligan KM (2016) Molecular evolution and functional diversification of replication protein A1 in plants. *Front Plant Sci* 7(33):33.
17. Ishibashi T, Kimura S, & Sakaguchi K (2006) A higher plant has three different types of RPA heterotrimeric complex. *J Biochem* 139(1):99-104.
18. Aklilu BB, Soderquist RS, & Culligan KM (2014) Genetic analysis of the Replication Protein A large subunit family in Arabidopsis reveals unique and overlapping roles in DNA repair, meiosis and DNA replication. *Nucleic Acids Res* 42(5):3104-3118.
19. Xia R*, et al.* (2006) ROR1/RPA2A, a putative replication protein A2, functions in epigenetic gene silencing and in regulation of meristem development in Arabidopsis. *Plant Cell* 18(1):85-103.
20. Elmayan T, Proux F, & Vaucheret H (2005) Arabidopsis RPA2: a genetic link among transcriptional gene silencing, DNA repair, and DNA replication. *Curr Biol* 15(21):1919-1925.
21. Kapoor A*, et al.* (2005) Mutations in a conserved replication protein suppress transcriptional gene silencing in a DNA-methylation-independent manner in Arabidopsis. *Curr Biol* 15(21):1912-1918.
22. MacAlister CA, Ohashi-Ito K, & Bergmann DC (2007) Transcription factor control of asymmetric cell divisions that establish the stomatal lineage. *Nature* 445(7127):537-540.
23. Pillitteri LJ, Sloan DB, Bogenschutz NL, & Torii KU (2007) Termination of asymmetric cell division and differentiation of stomata. *Nature* 445(7127):501-505.
24. Lee E, Lucas JR, Goodrich J, & Sack FD (2014) Arabidopsis guard cell integrity involves the epigenetic stabilization of the FLP and FAMA transcription factor genes. *Plant J* 78(4):566-577.
25. Melaragno JE, Mehrotra B, & Coleman AW (1993) Relationship between endopolyploidy and cell-size in epidermal tissue of Arabidopsis. *Plant Cell* 5(11):1661-1668.
26. Henricksen LA, Umbricht CB, & Wold MS (1994) Recombinant replication protein A: expression, complex formation, and functional characterization. *J Biol Chem* 269(15):11121-11132.
27. Harashima H & Schnittger A (2012) Robust reconstitution of active cell-cycle control complexes from co-expressed proteins in bacteria. *Plant Methods* 8:9.
28. Wang R*, et al.* (2016) The Brassinosteroid-Activated BRI1 Receptor Kinase Is Switched off by Dephosphorylation Mediated by Cytoplasm-Localized PP2A B Subunits. *Mol Plant* 9(1):148-157.
29. Din S, Brill SJ, Fairman MP, & Stillman B (1990) Cell-cycle-regulated phosphorylation of DNA replication factor A from human and yeast cells. *Genes Dev* 4(6):968-977.
30. Fang F & Newport JW (1993) Distinct roles of cdk2 and cdc2 in RPA phosphorylation during the cell cycle. *J Cell Sci* 106 (Pt 3)(3):983-994.

31. Binz SK, Sheehan AM, & Wold MS (2004) Replication protein A phosphorylation and the cellular response to DNA damage. *DNA Rep* 3(8-9):1015-1024.
32. Boudolf V*, et al.* (2004) B1-type cyclin-dependent kinases are essential for the formation of stomatal complexes in *Arabidopsis thaliana*.*Plant Cell* 16(4):945-955.
33. Magyar Z*, et al.* (2012) Arabidopsis E2FA stimulates proliferation and endocycle separately through RBR-bound and RBR-free complexes. *EMBO J* 31(6):1480-1493.
34. Boudolf V*, et al.* (2004) The plant-specific cyclin-dependent kinase CDKB1;1 and transcription factor E2Fa-DPa control the balance of mitotically dividing and endoreduplicating cells in Arabidopsis. *Plant Cell* 16(10):2683-2692.
35. Marwedel T*, et al.* (2003) Plant-specific regulation of replication protein A2 (OsRPA2) from rice during the cell cycle and in response to ultraviolet light exposure. *Planta* 217(3):457-465.
36. Dornreiter I*, et al.* (1992) Interaction of DNA polymerase alpha-primase with cellular replication protein A and SV40 T antigen. *EMBO J* 11(2):769-776.
37. Castellano MM, Boniotti MB, Caro E, Schnittger A, & Gutierrez C (2004) DNA replication licensing affects cell proliferation or endoreplication in a cell type-specific manner. *Plant Cell* 16(9):2380-2393.
38. Han SK, *et al.* (2018) MUTE directly orchestrates cell-state switch and the single symmetric division to create stomata. *Dev Cell* 45(3):303-315.e305.
39. Weimer AK, *et al.* (2018) Lineage- and stage-specific expressed CYCD7;1 coordinates the single symmetric division that creates stomatal guard cells. *Development* 145(6).
40. Porter AC (2008) Preventing DNA over-replication: a Cdk perspective. *Cell Division* 3(1):3.
41. Garcia V*, et al.* (2003) AtATM is essential for meiosis and the somatic response to DNA damage in plants. *Plant Cell* 15(1):119-132.
42. Ciccia A & Elledge SJ (2010) The DNA damage response: making it safe to play with knives. *Mol Cell* 40(2):179-204.
43. Yoshiyama KO*, et al.* (2013) ATM-mediated phosphorylation of SOG1 is essential for the DNA damage response in Arabidopsis. *EMBO Rep* 14(9):817-822.
44. Weimer AK*, et al.* (2016) The plant-specific CDKB1-CYCB1 complex mediates homologous recombination repair in Arabidopsis. *EMBO J* 35(19):2068-2086.
45. Xie Z, Li D, Wang L, Sack FD, & Grotewold E (2010) Role of the stomatal development regulators FLP/MYB88 in abiotic stress responses. *PlantJ* 64(5):731-739.
46. Eschbach V & Kobbe D (2014) Different replication protein A complexes of Arabidopsis thaliana have different DNA-binding properties as a function of heterotrimer composition. *Plant Cell Physiol* 55(8):1460-1472.
47. Weimer AK*, et al.* (2012) Retinoblastoma related1 regulates asymmetric cell divisions in Arabidopsis. *Plant Cell* 24(10):4083-4095.

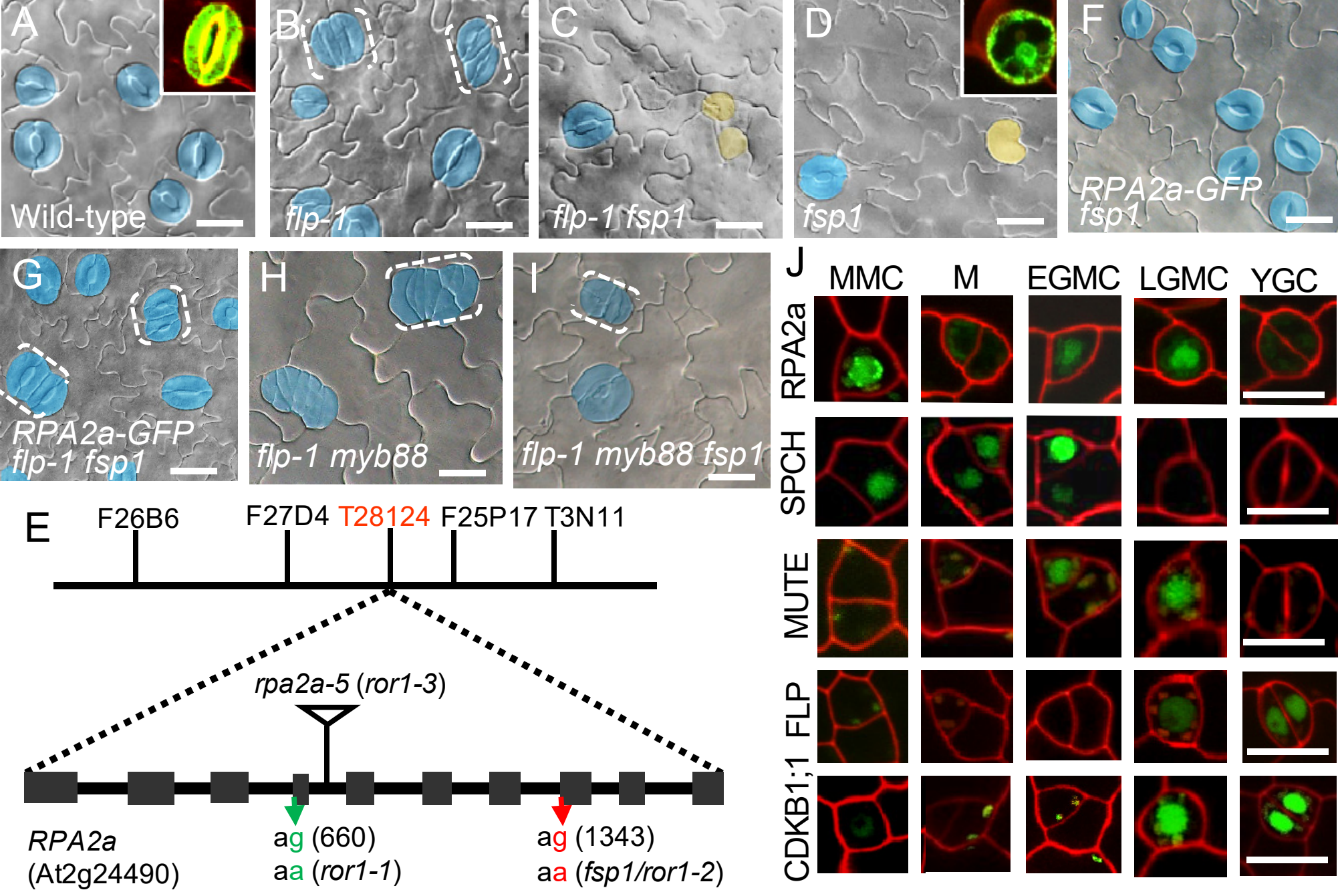
A
Wild-type
B
flp-1
C
flp-1 fsp1
D
fsp1
F
RPA2a-GFP
fsp1
G
RPA2a-GFP
flp-1 fsp1
H
flp-1 myb88
I
flp-1 myb88 fsp1
E
F26B6
F27D4
T28124
F25P17
T3N11
rpa2a-5 (ror1-3)
RPA2a
(At2g24490)
ag (660)
aa (ror1-1)
ag (1343)
aa (fsp1/ror1-2)
J
MMC
M
EGMC
LGMC
YGC
RPA2a
SPCH
MUTE
FLP
CDKB1;1

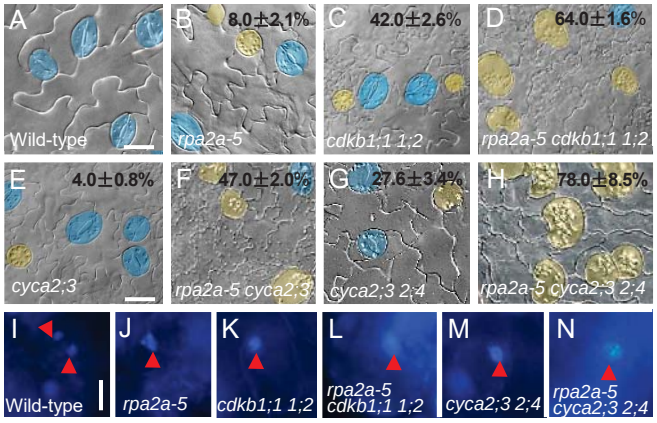
A
Wild-type
B
8.0±2.1%
rpa2a-5
C
42.0±2.6%
cdkb1;1 1;2
D
64.0±1.6%
rpa2a-5 cdkb1;1 1;2
E
4.0±0.8%
cyca2;3
F
47.0±2.0%
rpa2a-5 cyca2;3
G
27.6±3.4%
cyca2;3 2;4
H
78.0±8.5%
rpa2a-5 cyca2;3 2;4
I
Wild-type
J
rpa2a-5
K
cdkb1;1 1;2
L
rpa2a-5
cdkb1;1 1;2
M
cyca2;3 2;4
N
rpa2a-5
cyca2;3 2;4

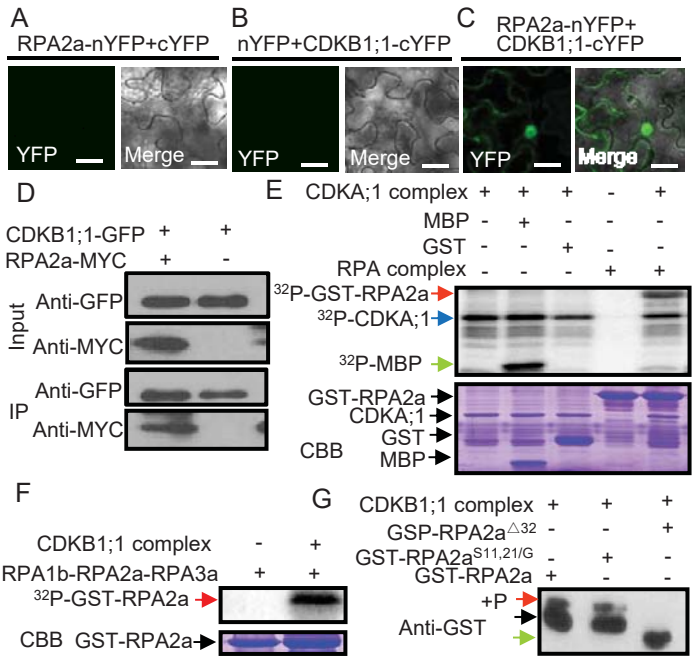
A
RPA2a-nYFP+cYFP
YFP
Merge
B
nYFP+CDKB1;1-cYFP
YFP
Merge
C
RPA2a-nYFP+
CDKB1;1-cYFP
YFP
Merge
D
CDKB1;1-GFP + +
RPA2a-MYC + -
Input
Anti-GFP
Anti-MYC
IP
Anti-GFP
Anti-MYC
E
CDKA;1 complex + + + - +
MBP - + - - -
GST - - + - -
RPA complex - - - + +
32P-GST-RPA2a
32P-CDKA;1
32P-MBP
GST-RPA2a
CDKA;1
GST
MBP
CBB
F
CDKB1;1 complex - +
RPA1b-RPA2a-RPA3a + +
32P-GST-RPA2a
CBB GST-RPA2a
G
CDKB1;1 complex + + +
GSP-RPA2a△32 - - +
GST-RPA2aS11,21/G - + -
GST-RPA2a + - -
+P
Anti-GST

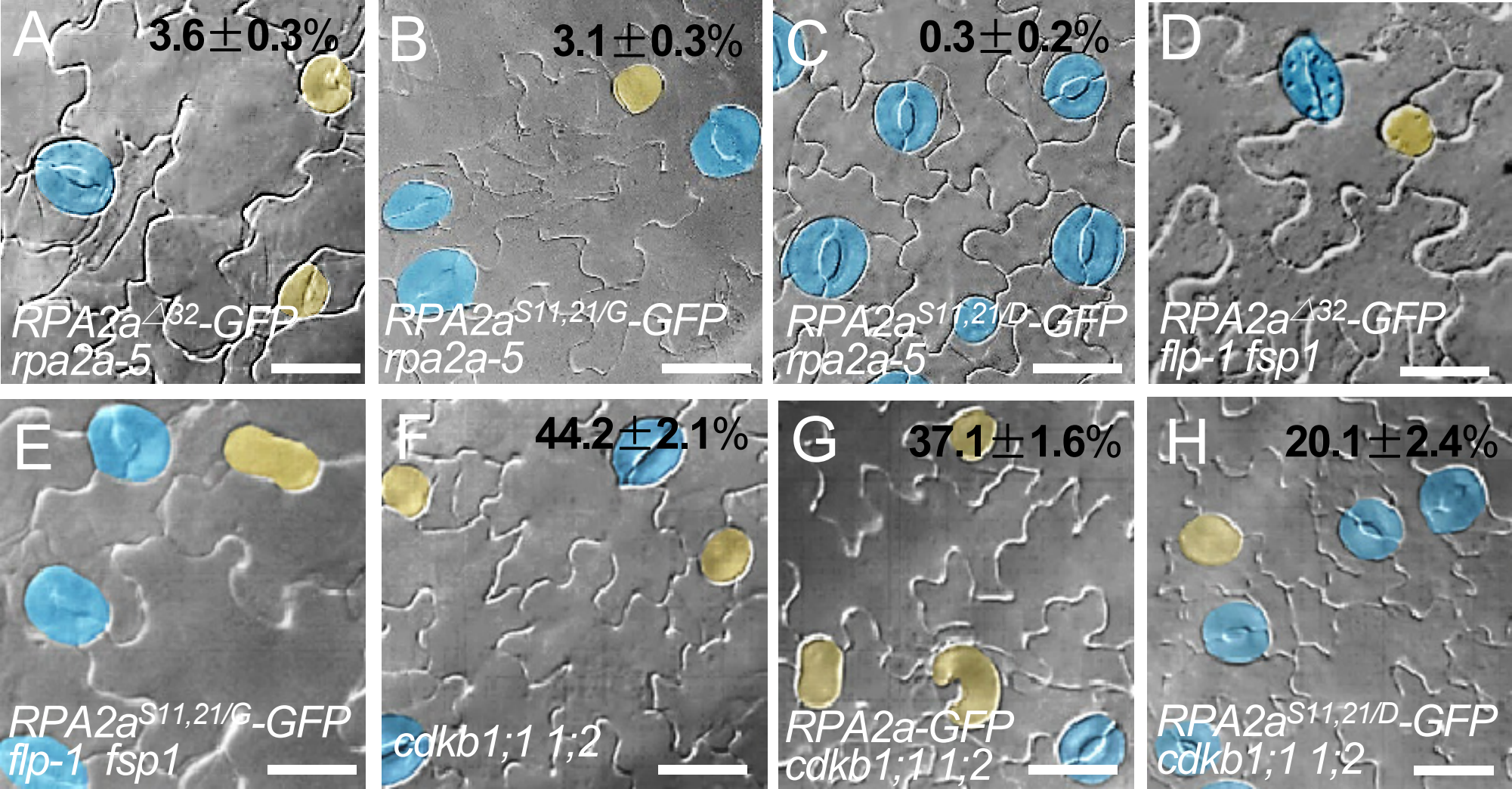
A
3.6±0.3%
RPA2a△32-GFP
rpa2a-5
B
3.1±0.3%
RPA2aS11,21/G-GFP
rpa2a-5
C
0.3±0.2%
RPA2aS11,21/D-GFP
rpa2a-5
D
RPA2a△32-GFP
flp-1 fsp1
E
RPA2aS11,21/G-GFP
flp-1 fsp1
F
44.2±2.1%
cdkb1;1 1;2
G
37.1±1.6%
RPA2a-GFP
cdkb1;1 1;2
H
20.1±2.4%
RPA2aS11,21/D-GFP
cdkb1;1 1;2

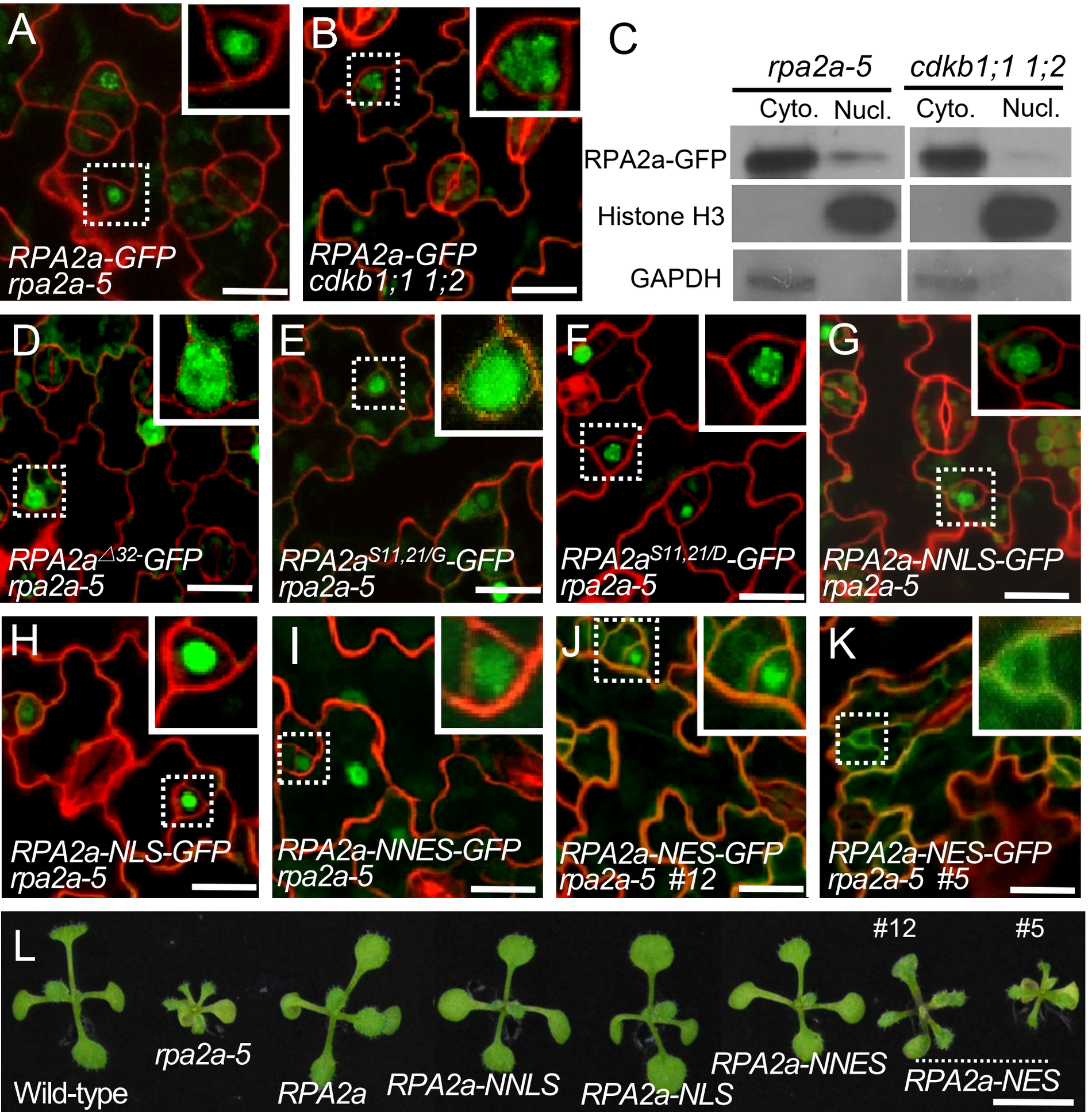
A
RPA2a-GFP
rpa2a-5
B
RPA2a-GFP
cdkb1;1 1;2
C
rpa2a-5
cdkb1;1 1;2
Cyto.
Nucl.
Cyto.
Nucl.
RPA2a-GFP
Histone H3
GAPDH
D
RPA2a△32-GFP
rpa2a-5
E
RPA2aS11,21/G-GFP
rpa2a-5
F
RPA2aS11,21/D-GFP
rpa2a-5
G
RPA2a-NNLS-GFP
rpa2a-5
H
RPA2a-NLS-GFP
rpa2a-5
I
RPA2a-NNES-GFP
rpa2a-5
J
RPA2a-NES-GFP
rpa2a-5 #12
K
RPA2a-NES-GFP
rpa2a-5 #5
L
#12
#5
Wild-type
rpa2a-5
RPA2a
RPA2a-NNLS
RPA2a-NLS
RPA2a-NNES
RPA2a-NES

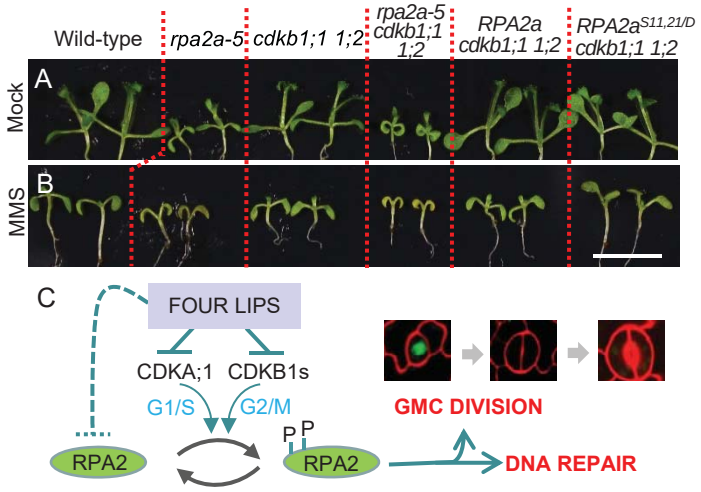
Wild-type
rpa2a-5
cdkb1;1 1;2
rpa2a-5 cdkb1;1 1;2
RPA2a cdkb1;1 1;2
RPA2a S11,21/D cdkb1;1 1;2
Mock
MMS
A
B
C
FOUR LIPS
CDKA;1
CDKB1s
G1/S
G2/M
RPA2
P P
RPA2
GMC DIVISION
DNA REPAIR